

This article was downloaded by:

On: 23 January 2011

Access details: *Access Details: Free Access*

Publisher *Taylor & Francis*

Informa Ltd Registered in England and Wales Registered Number: 1072954 Registered office: Mortimer House, 37-41 Mortimer Street, London W1T 3JH, UK



Journal of Coordination Chemistry

Publication details, including instructions for authors and subscription information:

<http://www.informaworld.com/smpp/title~content=t713455674>

Meridional anchorage of coordinate occupancy by a planar tridentate ligand and its effect on ligand substitution reactions of octahedral ruthenium(II) complexes

Felicia Tiba^a; Deogratius Jaganyi^a; Allen Mambanda^a

^a School of Chemistry, University of KwaZulu-Natal, Scottsville, 3209, South Africa

First published on: 09 August 2010

To cite this Article Tiba, Felicia , Jaganyi, Deogratius and Mambanda, Allen(2010) 'Meridional anchorage of coordinate occupancy by a planar tridentate ligand and its effect on ligand substitution reactions of octahedral ruthenium(II) complexes', *Journal of Coordination Chemistry*, 63: 14, 2542 – 2560, First published on: 09 August 2010 (iFirst)

To link to this Article: DOI: 10.1080/00958972.2010.507269

URL: <http://dx.doi.org/10.1080/00958972.2010.507269>

PLEASE SCROLL DOWN FOR ARTICLE

Full terms and conditions of use: <http://www.informaworld.com/terms-and-conditions-of-access.pdf>

This article may be used for research, teaching and private study purposes. Any substantial or systematic reproduction, re-distribution, re-selling, loan or sub-licensing, systematic supply or distribution in any form to anyone is expressly forbidden.

The publisher does not give any warranty express or implied or make any representation that the contents will be complete or accurate or up to date. The accuracy of any instructions, formulae and drug doses should be independently verified with primary sources. The publisher shall not be liable for any loss, actions, claims, proceedings, demand or costs or damages whatsoever or howsoever caused arising directly or indirectly in connection with or arising out of the use of this material.

Meridional anchorage of coordinate occupancy by a planar tridentate ligand and its effect on ligand substitution reactions of octahedral ruthenium(II) complexes†

FELICIA TIBA, DEOGRATIUS JAGANYI* and ALLEN MAMBANDA

School of Chemistry, University of KwaZulu-Natal, Scottsville, 3209, South Africa

(Received 24 March 2010; in final form 4 June 2010)

A kinetic study of the substitution behavior of octahedral $[\text{Ru}(\text{terpy})(\text{bipy})(\text{OH}_2)]^{2+}$ and $[\text{Ru}(\text{terpy})(\text{tmen})(\text{OH}_2)]^{2+}$ {terpy = 2,2':6',2''-terpyridine, bipy = 2,2'-bipyridine and tmen = *N,N,N',N'*-tetramethylethylenediamine} with thiourea, 1,3'-dimethyl-2-thiourea, and acetonitrile nucleophiles (Nu) as a function of concentration in pH of 4.0 aqueous media using UV-Vis spectroscopy has been made. The reactions are first order in both the concentration of the Nu and the ruthenium complex in accordance to the two-term rate law $k_{\text{obs}} = k_2[\text{Nu}] + k_{-2}$. The ligand effect of the *cis*-coordinated bidentates (NN) on the substitutional lability of the aqua leaving group in the $[\text{Ru}(\text{terpy})(\text{NN})(\text{OH}_2)]^{2+}$ complexes increases in the order: NN = dppro < dopro < phen \approx bipy < tmen < diox < Me₂phen. This order reflects the steric as well as the electronic properties of the bidentate ligand where the meridionally coordinated terpy enacts stereoelectronic rigidity on the bidentate ligand in addition to providing an efficient drainage of electron density at the metal centers. In the tmen complex, the retardation of the incoming groups caused by a dominant *cis* σ -effect from the tmen toward the metal center controls the rate of the reaction, as a result of the induced weakening of the scorpionatic effect of the steric tmen ligand due to the strong π -repulsive backbone of the meridionally coordinated terpy.

Keywords: Ruthenium(II); Octahedral; Ligand substitution; Terpy and Bidentate

1. Introduction

Despite heightened concern about the toxicity of metal-based therapeutics, these compounds have shown promising use in clinical pharmacology, particularly in the treatment of cancer, viral diseases, and antibiotic-resistant infections [1]. One of the leading metal-based drugs which has had a tremendous impact on cancer patients (especially those suffering from genitourinary tumors) has been *cis*-diaminedichloroplatinum(II), also known as cisplatin. However, severe side-effects, resistance, and its non-oral administration to patients have limited its widespread use in the clinic, stimulating a protracted search for new cytostatics.

One of the strategies in this wide-cast search for efficacious drugs has been to change the prototypal central metal ion, Pt(II), to other metal ions (such as ruthenium(II/III) [2, 3] and gold(III) [3]) in the Pt(II) complexes already showing promising antitumor

*Corresponding author. Email: jaganyi@ukzn.ac.za

†On the occasion of Professor Rudi van Eldik's 65th birthday.

activity, while maintaining the cisplatin's classical $cis\text{-}\{M^{n+}(\text{NH}_3)_2\}$ active phenotype on the cytostatics. Other potentially useful metal ions are rhenium(II), rhodium(I), osmium(II/III), and iridium(I). When the geometry of the platinum complexes is changed from square planar to octahedral, while maintaining the classical cis -geometry of the non-leaving groups, active antitumor cytotoxicities were afforded as prodrugs of cisplatin-like cytostatics [1]. This was also true for ruthenium. The most notable antitumor agent to come out of this approach is *trans*-[bis-(acetato)aminedichloro (cyclohexylamine)platinum(IV)], also known as sastraplatin or JM 216, which has potential for the treatment of ovarian and lung cancers [2]. Other successful agents were the octahedral ruthenium(III) complexes $cis\text{-}[\text{Ru(III)(NH}_3)_4\text{Cl}_2]\text{Cl}$; Na/HIm[*trans*-[Ru(III)(Im)(DMSO)Cl₄] [3] Im = Imidazole, DMSO = dimethyl sulfoxide; and *mer*-[Ru(terpy)Cl₃] [4 a] terpy = 2,2':6',2''-terpyridine, all of which have shown antitumor activity profiles similar to cisplatin especially against metastatic tumor growth. Intriguingly, ruthenium(III) octahedral complexes containing planar polypyridyl functional groups such as terpy, 2,2'-bipyridine, and 1,10-phenanthroline are not only chiral, but also offered valuable applications such as DNA structural probing [4a], DNA cleaving reagents [4b–d], biological switches [4e,f] as well as electron-transfer reagents [4g–j].

As part of our interest in synthesis and understanding substitutional reactivity of octahedral Ru(II) complexes, which contain a ligand backbone with potential to intercalate between DNA nucleobase pairs communal to the site of ligand substitution by N7 atoms of the DNA bases as well as having valuable photophysical and electrochemical properties, we studied and report herein the kinetics of two complexes, [Ru(terpy)(NN)H₂O]²⁺ {NN = 2,2'-bipyridine (bipy) and *N,N,N',N'*-tetramethylethylenediamine (tmen)}, with two sulfur donor nucleophiles [thiourea (TU), 1,3'-dimethyl-2-thiourea (DMTU)] and a nitrogen donor (acetonitrile) nucleophile as a function of nucleophile concentration at 298 K. In these complexes, the terpy ligand seems to anchor the coordinate occupancy of three of the equatorial positions in a meridional fashion, forcing the bidentate to coordinate *facially* with respect to the leaving group.

2. Experimental

2.1. Material and procedures

The following chemicals reagents: ethanol, acetonitrile (dried over 4 Å molecular sieves and purged with nitrogen before use), ethyltriamine (Et₃N), ethyl glycol, diethyl ether, and perchloric acid (70%) were analytical reagent grade and were used without purification. The solid chemicals such as silver perchlorate (99%), sodium perchlorate, ruthenium trichloride · trihydrate, lithium chloride, sodium perchlorate · monohydrate, terpy, (bipy), tmen, TU, and TMTU were purchased from Aldrich and used as supplied. Ultrapure water (MODULAB water purification system) was used in all aqueous synthetic and kinetic procedures. The precursor complex [Ru(terpy)Cl₃] was synthesized as previously described [5]. The cations [Ru(terpy)(bipy)(Cl)]⁺ [6] and [Ru(terpy)(tmen)(Cl)]⁺ [7] were synthesized following procedures reported in the literature with minor modifications in the purification steps. The complexes were precipitated as their chloro as well as perchlorate salts and were characterized by FT-IR spectroscopy (Perkin–Elmer spectrum One), UV-Vis spectroscopy, microanalysis

(Carlo Erba Elemental Analyser 1106), and ^1H NMR (500 MHz Varian Unity Inova). The IR (Figure SI 1 a,b, ESI) and NMR spectroscopic (Figure SI 1 c,d, ESI) data agreed with those from the earlier preparations.

[Ru(terpy)(bipy)(Cl)](ClO₄): ^1H NMR (500 MHz, CD₃CN) δ (ppm): 10.2 (d, $J_{5-6} = 5.54$ Hz, H₆ *bipy*); 8.63 (d, $J_{3'-4'} = 8.00$ Hz, H₃ *bipy*) 8.52 (d, $J_{e-f} = 8.00$ Hz, H_e *tpy*); 8.42 (d, $J_{d-c} = 8.00$ Hz, H_d *tpy*); 8.28 (m, $J_{4-5} = 8.00$ Hz, H₄ *bipy*); 8.12 (m, $J_{e-f} = 8.00$ Hz, H_f *tpy*); 7.97 (m, $J_{5-4} = 8.31$ Hz, H₅ *bipy*); 7.71 (ddd, $J_{c-d} = 8.00$ Hz, $J_{c-d} = 8.00$ Hz, H_c *tpy*); 7.68 (d, $J_{a-b} = 5.54$ Hz, H_a *tpy*); 7.33 (d, $J_{6'-5'} = 4.93$ Hz, H₆ *bipy*); 6.95 (m, $J_{b-c} = 8.00$ Hz, H_b *tpy*).

[Ru(terpy)(tmen)Cl]ClO₄·0.2NaClO₄: Yield: 167.2 mg. ^1H NMR (500 MHz, CD₃CN) δ (ppm): 9.13 (d, 2H, H_a *tpy*); 8.40 (d, 4H, H_d + _g *tpy*); 8.02 (d, 2H, H_c *tpy*); 7.86 (m, 2H, H_h *tpy*); 7.67 (m, 2H, H_b *tpy*); 3.42 (s, 6H, H₄ *tmen*); 3.28 (m, 2H, H₃ *tmen*); 2.62 (m, 2H, H₂ *tmen*); 1.33 (s, 6H, H₁ *tmen*). Microanalysis Calcd for [Ru(terpy)(tmen)Cl]ClO₄·0.2NaClO₄ (%): C, 41.35; H, 4.46; N, 11.48. Found (%): C, 41.37; H, 4.41; N, 11.40. UV-Vis (CH₂Cl₂) [λ_{max} , nm (ϵ , (mol L⁻¹)⁻¹ cm⁻¹)]: 563 (3049.594) sh, 380 (3003.216) br, 326 (21869.976) br, 281 (27067.627) br, where br = broad; sh = shoulder.

To obtain the desired aqua derivatives of the Ru(II) complexes, their chloro salts, [Ru(terpy)(tmen)(Cl)]Cl and [Ru(terpy)(bipy)(Cl)](Cl), were reacted with 1.99 equivalents of AgClO₄ in 20 mL of acetone/water (3 + 1) and the mixture left to reflux for 1 h. The AgCl precipitate that formed was filtered using a Millipore filtration system fitted with 0.1 μM pore membrane filter. The filtrate was concentrated under reduced pressure from which brown-black crystalline powder of the desired product was formed through slow evaporation. The powder was collected by filtration, washed with small amounts of cold water, and then dried *in vacuo* in the case of ([Ru(terpy)(bipy)(H₂O)]ClO₄) and a solution of known concentration for [Ru(terpy)(tmen)(H₂O)]ClO₄.

Yield: [Ru(terpy)(bipy)(OH₂)](ClO₄)₂: 0.0250 g (0.035 mmol, 44%); Calcd for RuC₂₅H₂₁N₅O₉Cl₂ (%): C, 42.44; H, 2.69; N, 9.9. Found (%): C, 42.29; H, 2.61; N, 9.95; UV-Vis (H₂O) [λ_{max} , nm (ϵ , (mol L⁻¹)⁻¹ cm⁻¹)]: 475 (8742.594) br; 312 (33226.897) br; 288 (34200.674) br; 231 (24045.912) sh, where br = broad; sh = shoulder.

2.2. Physical measurements and instrumentation

2.2.1. Determination of the $\text{p}K_{\text{a}}$ of the octahedral Ru(II) complexes. To probe the acidity of the complexes, the two ruthenium(II) complexes were titrated spectrophotometrically with NaOH at 25°C. The details of the titration procedure are reported in our previous article [8]. The pH of the solution was measured on a Jenway 4330 pH meter station having a combination Jenway glass electrode that had been calibrated using standard buffer solutions at pH 4.0, 7.0, and 10.0 (Merck). To avoid precipitation of KClO₄ in the pH electrode, the KCl solution inside the electrode was replaced with 3 mol L⁻¹ NaCl [8a]. The UV-Vis spectrum acquired at each pH was recorded using a Cary 100 UV-Vis Spectrophotometer (Varian). To calculate the $\text{p}K_{\text{a}}$ values of the complexes, the absorbance/pH data were fitted using Origin 5.0 to a standard equation (1)

$$\text{Abs} = \left(K - \frac{[\text{H}^+]\text{K}}{K_{\text{a}} + [\text{H}^+]} \right) \alpha + \left(\frac{[\text{H}^+]\text{K}}{K_{\text{a}} + [\text{H}^+]} \right) \beta \quad (1)$$

where $[H^+]$ is the concentration of protons and can be expressed as 10^{-pH} , K_a is the acid dissociation constant and can be written as 10^{-pK_a} , K is the fraction of the $[H^+]$ and $[OH^-]$ in the solution with maximum value of 1, and α and β are the upper and lower limits of absorbance, respectively.

2.2.2. Computational details. Density functional theoretical (DFT) [9 a,b] calculations were performed with the Spartan'04 for Windows quantum chemical package [9c,d] using the B3LYP method, [9e,f] a three parameter hybrid functional procedure, utilizing the LACVP +** [9g,h] pseudo potentials basis set. Key calculated geometrical data and structures are summarized in tables 1 and 2, respectively.

2.2.3. Ligand substitution reactions of octahedral ruthenium(II) complexes. All ligand substitution reactions were performed under pseudo first-order conditions with the concentration of the nucleophiles being present in at least 100-fold excess over that of the metal complexes. This ensured that the reactions go to completion. The wavelengths chosen (where a biggest change in the absorbance was recorded) for the kinetic reactions were initially determined using UV-Vis absorption spectra collected over the range 800–200 nm, from experiments run on a Cary 100 Bio UV-Vis spectrophotometer (Varian) with an attached thermostated cell holder controlled by a Varian Peltier temperature-control unit. The temperature of the cell holder was controlled to an accuracy of $\pm 0.05^\circ\text{C}$ and 0.1°C . All reactions were followed for at least six half-lives. Data were acquired and analyzed using an online kinetic application. The wavelengths

Table 1. Summary of DFT [9 a, b] calculated data for $[\text{Ru}(\text{terpy})(\text{NN})\text{OH}_2]^{2+}$, NN = bipy; phen; 2,9-Me₂phen and tmen.

Property	NN=bipy	phen	2,9-Me ₂ phen	tmen
Bond lengths (Å)				
Ru–Cl	2.438	2.433	2.457	2.421
^a Ru–N _{ne1} terpy	2.113	2.112	2.129	2.123
^b Ru–N _c terpy	1.992	1.990	1.990	1.981
Ru–N _{ne2} terpy	2.114	2.114	2.104	2.137
Ru–N' _{trans} bipy	2.104	2.114	2.161	2.186
Ru–N' _{cis} bipy	2.126	2.136	2.197	2.203
Separation distance (Å)				
H' _{(NN)proximal} –Cl	2.546	2.627	–	–
H' _{NH2(NN)} –Cl	–	–	–	3.103
H' _{CH3(NN)} –Cl	–	–	2.632	2.585
Bond angles (°)				
N' _{trans} bipy–Ru–Cl	171.1	171.1	174.5	166.2
N _c terpy Ru–N _{nc} terpy	79.79	79.09	79.4	78.8
N _{nc} terpy Ru–N _{nc} terpy	157.9	158.1	158.3	155.9
Energy gap (eV)				
LUMO energy (eV)	–4.84	–4.79	–4.79	–4.85
HOMO energy (eV)	–7.77	–7.72	–7.71	–7.70
$\Delta E_{\text{LUMO-HOMO}}$	2.93	2.93	2.92	2.85
Natural charges				
Ru ²⁺	0.914	0.913	0.904	0.887

N_c = nitrogen of the central ring, N_{nc} = nitrogen of the central ring.

^aN of the non-central terpy ring.

^bN of the central terpy ring.

used for $[\text{Ru}(\text{terpy})(\text{bipy})\text{H}_2\text{O}]^+$ were 458, 455, and 371 nm with respect to TU, DMTU, and CH_3CN nucleophiles, respectively. Reactions between $[\text{Ru}(\text{tmen})(\text{bipy})\text{H}_2\text{O}]^+$ and TU, DMTU, and CH_3CN nucleophiles were monitored at 451, 371, and 386 nm, respectively.

Kinetic studies were monitored spectrophotometrically by collecting repetitive spectral scans of the reaction mixture or by monitoring the kinetic reaction at a specific wavelength. All the spectral changes are associated with the disappearance of the starting complex. For all the reactions, the final spectra had well-defined differences from that of the starting aqua complexes, namely, $[\text{Ru}(\text{terpy})(\text{bipy})\text{H}_2\text{O}]^+$ and $[\text{Ru}(\text{tmen})(\text{bipy})\text{H}_2\text{O}]^+$ and were that of the substituted products, namely, $[\text{Ru}(\text{terpy})(\text{bipy})\text{Nu}]^+$ and $[\text{Ru}(\text{tmen})(\text{bipy})\text{Nu}]$, respectively.

3. Results

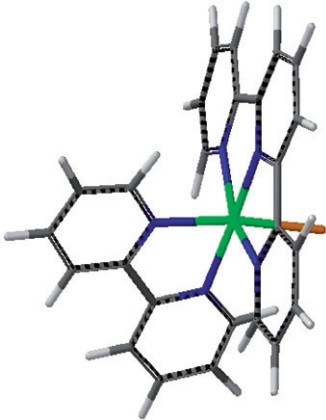
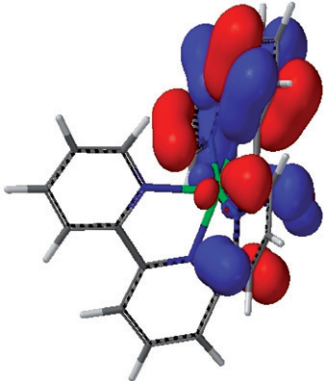
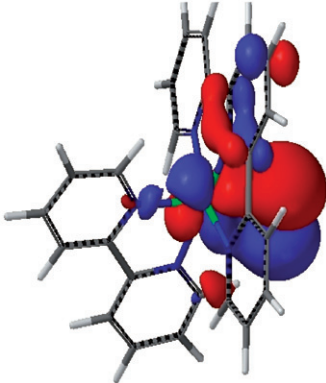
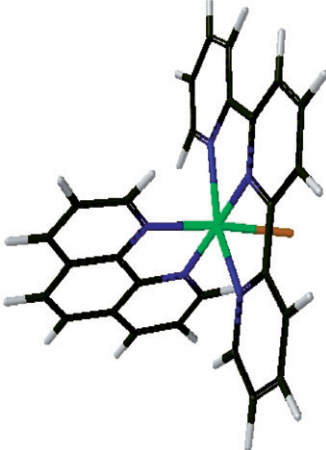
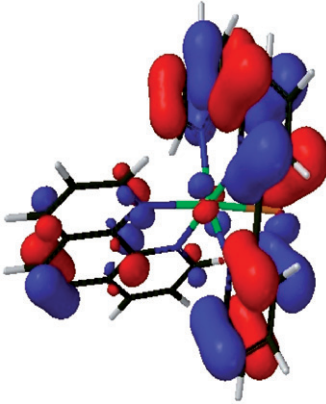
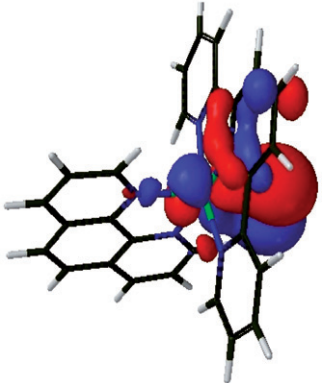
3.1. Computational calculations

In order to understand the structural as well as the electronic properties in the two complexes, we modeled the complexes using the B3LYP/LACVP +** method [9]. Included in the modeling, for the purpose of extending this understanding, are two analogous complexes, namely, the phen and the 2,9-Me₂phen derivatives. An extract of their calculated data, geometry-optimized structures, and frontier molecular orbitals are presented in tables 1 and 2, respectively.

The geometry-optimized structures in table 2 reveal that all bidentate ligands are *cis*-coordinated at the octahedral ruthenium(II) metal center, while the terpy (*mer*-terpy) is coordinated meridionally along the equatorial plane [10 a]. Three coordination sites at ruthenium were maintained constant by the *mer*-terpy chelating ligand, which exerts steric repulsive forces from its extended π -electron cloud toward the *cis*-coordinated bidentate ligands. Thus, the meridional terpy anchors the bidentate ligands at the metal center in an orthogonal plane, such that one of the coordinative arms of the bidentate ligand is always positioned *trans* to the aqua leaving group (table 2). The primary role of the terpy is, thus, to maintain some degree of stereoelectronic rigidity in the bidentate ligands, forcing significant, and mutual structural distortions in the planarity of the terpy as well as the diimine bidentate, particularly in the complexes with substituted bidentate ligands. The distorting forces depend on the steric bulk, location, and overall steric topology of the ancillary groups on the skeleton of the diimine and diamine bidentates.

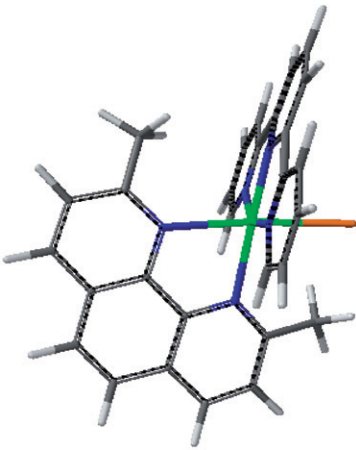
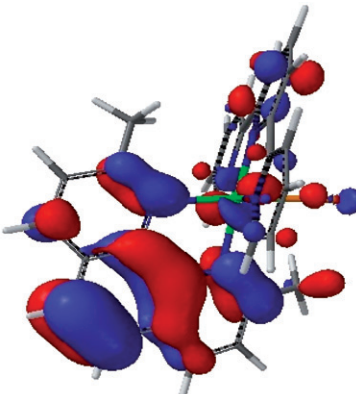
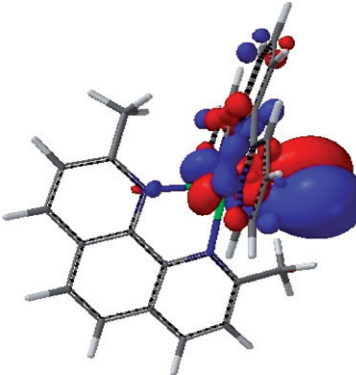
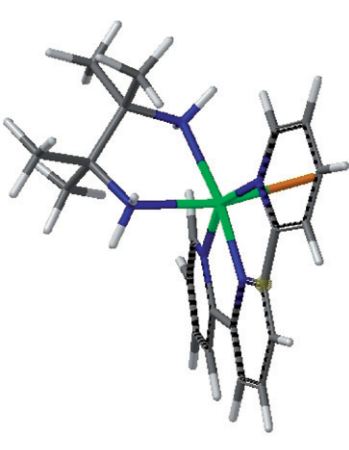
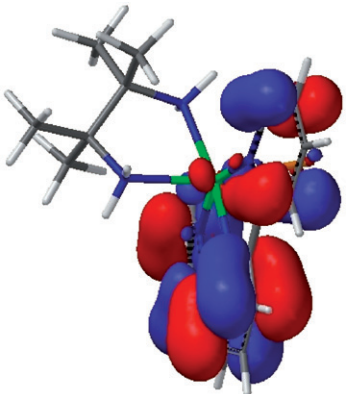
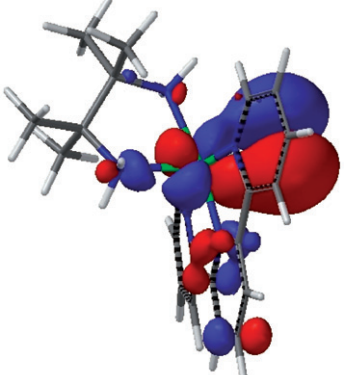
Stereoelectronic rigidity of the *cis*-coordinated bidentate ligands causes special types of interactions which have been collectively referred to in literature as the in-plane ligand effect (IPLE) [10 b]. The repulsive forces of the interactions are exerted on the leaving groups (the active sites) by closely positioned atoms or ancillary groups on the bidentate backbone. The origins of these interactions are predominantly steric. Depending on the steric topology of these atoms or ancillary groups on the bidentate ligand, their electron clouds repel those of the other coordinated ligands including the anchoring terpy, causing proportional distortions in the structures of the ligands or the bonding metrics around the octahedral geometry.

Table 2. DFT [9 a, b] minimum energy structures, HOMO and LUMO frontier molecular orbitals for $[\text{Ru}(\text{terpy})(\text{NN})\text{OH}_2]^{2+}$, NN = bipy; phen; 2,9-Me₂phen and tmen complexes.

Bidentate (NN)	Structure	HOMO Map	LUMO Map
bipy			
phen			

(Continued)

Table 2. Continued.

Bidentate (NN)	Structure	HOMO Map	LUMO Map
2,9-Me₂phen			
tmn			

The calculations were performed with the Spartan'04 for Windows quantum B3LYP hybrid functional method [9 e, f] utilizing the LACVP+** [9 g, h] pseudopotentials basis set.

Repulsive interactions between the co-ligand and the consequent distortions suffered in their structures (the terpy, bidentate, and the leaving groups) are best illustrated in the geometry-optimized structures of tmen and 2,9-Me₂phen, two derivatives which have specially positioned steric-imparting ancillary groups on their bidentate ligands (table 2). In the model structure of the 2,9-Me₂phen complex, the distortions in the planarity of both the terpy and the 2,9-Me₂phen ligands are identifiable; the repulsive forces, induced by the extended π -electron cloud of the terpy, repel the two axially projected methyl groups on C2 and C9 of the bidentate off the axial plane. The strong repulsive forces of the two projected methyl groups cause tipped-down distortions on the peripheral pyridyl rings when referenced to the mean plane of the ligand, forcing the terpy into a conformation resembling the tipped-down wings of a hawk jet. The mutual repulsive forces from the extended π -electronic cloud of the *mer*-terpy onto the two axial methyl groups on phen causes a similar sideways tip-off of the peripheral rings of the 2,9-Me₂phen. The 2,9-Me₂phen also assumes a tipped-down conformation similar to that of the terpy but oriented sideways relative to the chloride leaving group. The distortions suffered on the planarity of the terpy are expected to reduce its π -acceptance of electron density from the metal center to some extent. It can also restrict the approach of the nucleophiles in the direction locating the leaving group. In addition, the configuration of the bidentate ligand when referenced to the plane of the terpy deviates from the expected near-orthogonality. This kind of rearrangement in the configuration of the ligand is necessary to minimize the strong electrostatic repulsive forces from the ancillary groups. As a result, the two methyl groups which are nearly eclipsed in the optimized structure are located 5.00° from colinearity of N'_{trans bipy}, Ru, and Cl, while the axial leaving chloride lies in an anti-configuration at an angle of about 4.29° from colinearity. Thus, the metrics of bonds around the octahedral geometry is more distorted in 2,9-Me₂phen than in the bipy analog making this complex highly reactive.

Even in the optimized structure of the tmen, where the steric ancillary groups are located on the hind side in the facial coordination at the metal center, the interactions are still strong and cause noticeable distortions on the planarity of the peripheral rings of the terpy. The steric topology of the four ancillary methyl groups of the tmen complex causes a similar distortion in planarity of the terpy as caused by 2,9-Me₂phen. However, the flexibility of the ligand averts the same kind of strain in the tmen ligand as well as the octahedral geometry as observed in the model structure of the 2,9-Me₂phen complex. Distortions are averted through flexible adjustments in bite angle at the metal center as well as its conformational angles of carbon. For example, the tetrahedral angle of Ru-N_{tmen}-C_{tmen} measures 114° in the model calculations.

In the unsubstituted bipy complex, however, the bidentate ligand lies in a bisector plane to the terpy and its hydrogens are nearly eclipsed with the axially positioned chloride leaving group. To minimize the repulsive forces between its hydrogens and the extended π -electron cloud, the central pyridyl ring of terpy assumes a slight tipped-down conformation (1.20°) relative to the mean plane of the ligand. This in turn repels the axial chloride ligand forcing it into a 1.79° inclination off the colinearity of the N'_{trans bipy}, Ru(II), and Cl. However, the planarity of bipy is hardly affected. A similar distortion on the central ring of the terpy is observed when the conjugated rings of the bidentate ligand are increased to three in the unsubstituted phen complex.

Table 3. The X-ray diffraction metric data of [Ru(II)(terpy)(phen/bipy)X] and the DFT calculated data of [Ru(II)(terpy)(phen/tmen)Cl]⁺ complexes.

Complex	Ru–N _{nc1} terpy	Ru–N _c terpy	Ru–N _{nc2} terpy	N _{nc1} terpy–Ru–N _{nc2} terpy	Reference
phen-H ₂ O	2.077	1.957	2.087	158.5	[9]
phen-H ₂ O	2.062	1.959	2.064	158.1	[10 a]
phen-Cl	2.070	1.967	2.077	158.7	[11 a]
bipy-Cl	2.087	1.989	2.087	158.3	[12], [12], [14]
bipy-NCCH ₃	2.060	1.937	2.064	154.8	[11 b] [14]
bipy	2.113	1.992	2.113	157.9	Calculated
2,9-Me ₂ Phen	2.123	1.990	2.129	158.3	Calculated
tmen	2.104	1.981	2.137	155.9	Calculated

Again, the planarity of phen was not affected. Minimum distortions on the planarity of the terpy ligands in model structures of the bipy and phen, near perfect octahedral geometry, and minimum change in the configuration of the bidentate ligand indicate that the electrostatic repulsive forces in these complexes where their bidentate ligands are unsubstituted are weak. A look at the metrics about the octahedral coordination sphere in the unsubstituted derivatives confirms that the bond angles and lengths remain within the range reported for other Ru(terpy)(NN)(X)]⁺ complexes. As documented in table 1, the calculated Ru–N_c terpy (N_c = nitrogen of the central ring) bond lengths for the complexes ranges from 1.990 to 1.996 Å and fall within the range measured of other Ru(terpy)(NN)(X)]⁺ (NN = bipy or phen) cations in the solid by X-ray diffraction analysis [10 a], and are always shorter [11] than the Ru–N_{nc} terpy (N_{nc} = nitrogen of the non-central ring) which was calculated in the range 2.123–2.137 Å. The calculated Ru–N_{nc} terpy bond lengths are, however, slightly longer than those measured in the solid which range between 2.060 and 2.086 Å [11]. The noticeable contraction of about 0.1 Å on the Ru(II)–N_c bond length of terpy has been reported before [11] and is due to the steric constraints imposed on the ligand upon coordination. As a result of the strain imposed on terpy, bite angles of the terpyridine reduces to an average value of ~79° in the complexes making an average angle of 159° in N_{nc} terpy–Ru(II)–N_{nc} terpy bond angle which should be ideally 180°. For the purpose of making a comparison, some bond lengths and angles have been listed in table 3.

The calculated data for the rigid bipy and the phen analogues are in good agreement with those reported for analogous complexes [Ru(terpy)(bipy)(OH₂)](ClO₄) [10 a, 11], [Ru(terpy)(phen)(Me)]PF₆ [10 a], and [Ru(terpy)(bipy)(CH₃CN)](PF₆)(ClO₄) · CH₃CN [11 b], where there is π-back bonding between the π-acceptors and central metal orbitals [10–15].

3.2. Determination of pK_a of the octahedral Ru(II) complexes

Absorption spectra of the two aqua complexes of ruthenium in aqueous pH 1.0 (HClO₄) solution are similar and characterized by a broad intense band at λ = 475 nm, ε = 8742 (mol L⁻¹)⁻¹ cm⁻¹ which is characteristic for a metal-to-ligand charge transfer {dπ (M) → π* of polypyridyl} transition. Further, as shown in figure 1, the UV-Vis spectra consist of several other intense bands in the UV region (200 < λ < 300 nm)

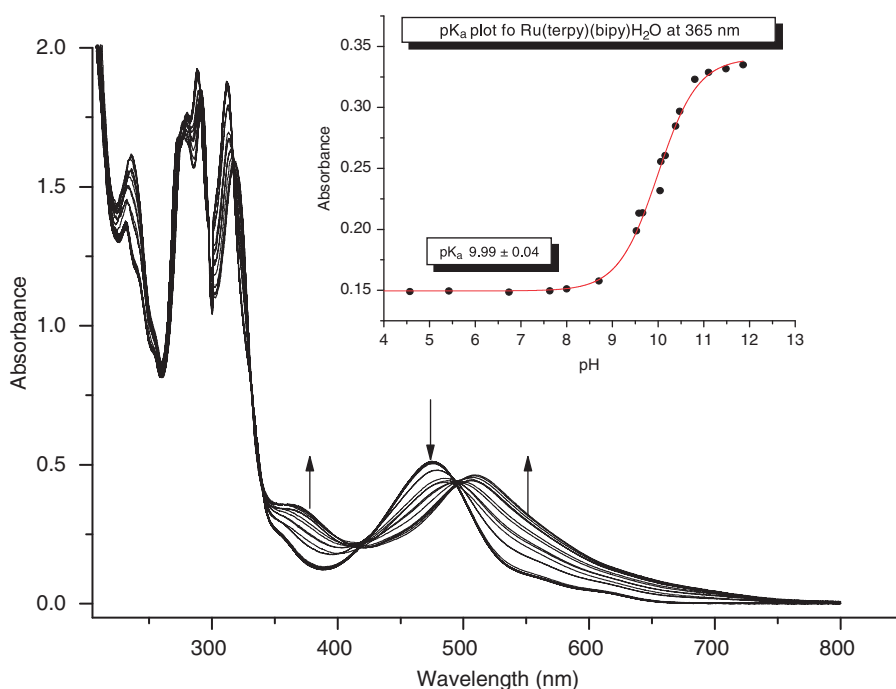
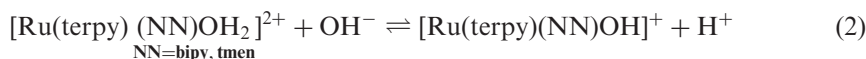


Figure 1. UV-Vis spectra of [Ru(terpy)(bipy)OH₂]²⁺ in the pH range 1–10 at 25°C, $\mu = 0.1 \text{ mol L}^{-1}$ (NaClO₄). Inset: The absorbance profile of [Ru(terpy)(bipy)OH₂]²⁺ at $\lambda = 365 \text{ nm}$.

which are assigned to polypyridyl $\pi \rightarrow \pi^*$ transitions [12, 16]. Typical UV-Vis stacked spectra, recorded during the titrations, are given for [Ru(terpy)(bipy)(OH₂)] in figure 1. The titration can be represented by equation (1).



When the pH 1.0 (HClO₄) solution was spectrophotometrically titrated with a solution of NaOH, the major band at 475 nm red-shifted to a wavelength of about 520 nm as the solution became basic with a slight initial loss in peak intensity. The red-shift is due to the destabilization of the $d\pi$ (M) orbitals to the electron-rich hydroxo when compared to the aqua. This causes a reduction in the energy gap of frontier orbitals $\{d\pi$ (M) \rightarrow π^* (polypyridyl)} resulting in the transitions of lower energy.

A fit of the absorbance data to a standard equation for determining the pK_a of monoprotic acids is shown as an inset for [Ru(terpy)(bipy)(OH₂)] in figure 1. The pK_a of [Ru(terpy)(bipy)OH₂]²⁺ and [Ru(terpy)(tmen)OH₂]²⁺ were determined to be 9.99 ± 0.04 and 10.27 ± 0.04 , respectively. These values are comparable to the respective values of 9.7 and 10.2, determined electrochemically [16]. The difference between the basicities confirms that tmen is a better σ -donor at the metal center.

The aqua forms of the two complexes dominate at lower pH values (1–7), while at higher pH values (>10) the hydroxo form is dominant. The titration processes were reversed when HClO₄ was added to the hydroxo form of the complexes. The titration curves are characterized by two isosbestic points, an indication that only the hydroxo

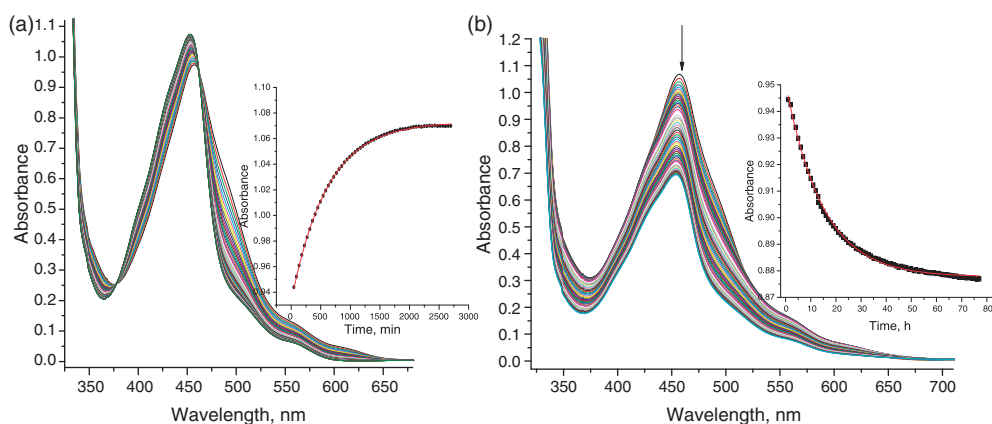


Figure 2. UV-Vis spectra recorded for the reactions of $[\text{Ru}(\text{terpy})(\text{bipy})\text{OH}_2]^{2+}$ with (a) CH_3CN and (b) TU in pH 4.0 (NaClO_4) aqueous solution, $T=25^\circ\text{C}$. Insets are the corresponding kinetic plots for the reactions at $\lambda = 451$ and 371 nm, respectively.

and the aqua species are present in the solution during titration as represented by equation (2).

3.3. Reactions of $[\text{Ru}(\text{terpy})(\text{NN})\text{OH}_2]^{2+}$, $\text{NN} = \text{bipy}; \text{tmen}$ with CH_3CN , TU, and DMTU

The octahedral ruthenium(II) complexes and nucleophiles TU, DMTU, and CH_3CN used in the kinetic analyses were dissolved in pH 4.0 (HClO_4) solutions whose ionic strength had been adjusted to 0.1 mol L^{-1} with NaClO_4 . The perchlorate is a non-coordinating ligand [17]. Thus, substitution of the coordinated aqua ligands of the complexes by the nucleophiles is given by equation (3).



The rates of substitution of the coordinated aqua were monitored spectrophotometrically by following the change in absorbance as a function of time under pseudo-first-order conditions using UV-Vis spectroscopy. Typical spectral changes accompanying the reactions between $[\text{Ru}(\text{terpy})(\text{bipy})\text{OH}_2]\text{ClO}_4$ and CH_3CN as well as $[\text{Ru}(\text{terpy})(\text{tmen})\text{OH}_2]\text{ClO}_4$ and TU are shown in figure 2 a and b, respectively. The corresponding kinetic traces taken at 371 and 451 nm are shown as insets in their respective figures.

All the kinetic traces obtained gave excellent non-linear least-square fits to a first-order exponential decay function. When the mean pseudo first-order rate constants representing four kinetic runs were plotted against the concentration of the incoming nucleophiles, linear plots that pass through zero were obtained in the case of the bipy complex as shown in figure 3, while non-zero y -intercepts were recorded in the concentration plots for the reactions of the tmen derivative (figure 4), suggesting

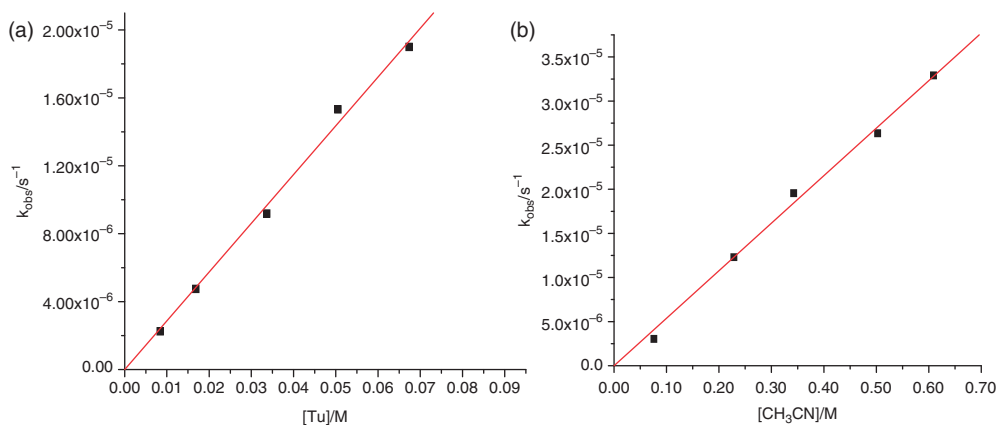


Figure 3. Plots of k_{obs} against the concentration of (a) TU and (b) CH₃CN nucleophiles for reaction between [Ru(terpy)(bipy)OH₂]²⁺ and (a) TU; (b) CH₃CN and (c) DMTU, pH = 4 (HClO₄), $\mu = 0.1 \text{ mol L}^{-1}$ (NaClO₄), $T = 25^\circ\text{C}$.

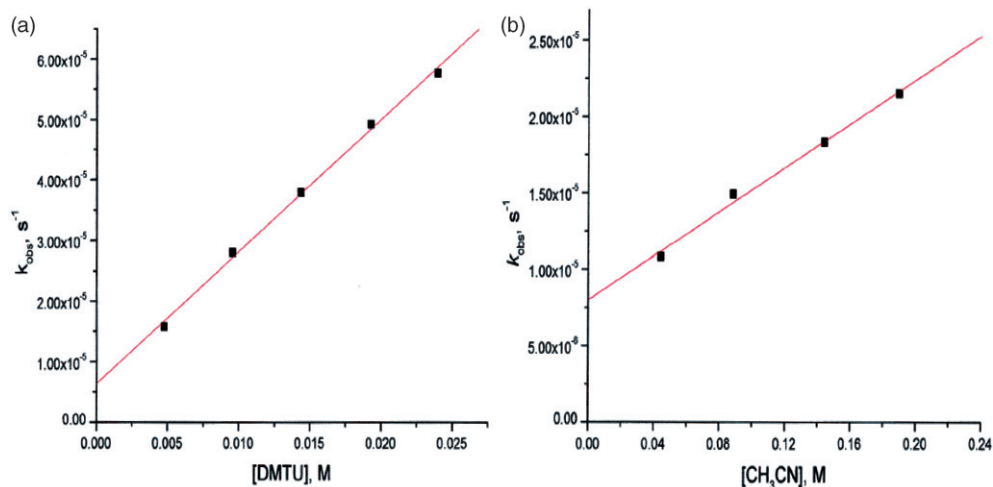


Figure 4. Plots of k_{obs} against the concentration of (a) DMTU and (b) CH₃CN nucleophiles for reaction between [Ru(terpy)(tmen)OH₂]²⁺, pH = 4.0 (HClO₄), $\mu = 0.1 \text{ mol L}^{-1}$ (NaClO₄), $T = 25^\circ\text{C}$.

that the substitution reactions of these complexes are first-order in the concentration of both Nu and Ru(II) complex in accordance to the rate law is given by equation (4):

$$k_{obs} = k_2[\text{Nu}] + k_{-2} \quad (4)$$

The zero intercepts recorded for reactions of [Ru(terpy)(bipy)OH₂]²⁺ with nucleophiles implies that the k_{-2} term in equation (4) is practically zero for its reactions. Thus, the rate law for substitution reactions in this complex by the nucleophiles simplifies to $k_{obs} = k_2[\text{Nu}]$. However, a back reaction is observed in reactions for the tmen complex and the nucleophiles (figure 4). The differences in reversibility of the reactions of these two complexes are possibly due to differences in the structural

Table 4. Second-order rate constants and the corresponding standard deviations for substitution of the coordinated aqua in ruthenium(II) by TU, DMTU, CH₃CN nucleophiles.

Complex	Nu	k_2 (10^{-4} (mol L ⁻¹) ⁻¹ s ⁻¹)	Ref.
[Ru(terpy)(bipy)OH ₂] ²⁺	TU	5.9 ± 0.10	This work
	DMTU	15.0 ± 0.30	This work
	CH ₃ CN	1.1 ± 0.02	This work
	CH ₃ CN	0.8 ± 0.05	[13]
[Ru(terpy)(tmen)OH ₂] ²⁺	TU	10.6 ± 0.30 (0.07 ± 0.003) ^a	This work
	DMTU	21.9 ± 0.70 (0.06 ± 0.01) ^a	This work
	CH ₃ CN	0.82 ± 0.04 (0.08 ± 0.005) ^a	This work
[Ru(terpy)(phen)OH ₂] ²⁺	CH ₃ CN	0.62 ± 0.01	[18]
[Ru(terpy)(Me ₂ phen)OH ₂] ²⁺	CH ₃ CN	410 ± 10	[18]
[Ru(terpy)(diox)(OH ₂)] ²⁺	CH ₃ CN	0.14 ± 0.01	[18]
[Ru(terpy)(dopro)(OH ₂)] ²⁺	CH ₃ CN	0.46 ± 0.01	[18]
[Ru(terpy)(dppro)(OH ₂)] ²⁺	CH ₃ CN	0.06 ± 0.001	[18]
[Ru(tpmm)(dppro)(OH ₂)] ²⁺	CH ₃ CN	1100000 ± 1000	[18, 20 a]

Standard deviations obtained for k_2 are those of the slope of the plot of k_{obs} versus nucleophile concentration.

^a k_{-2} .

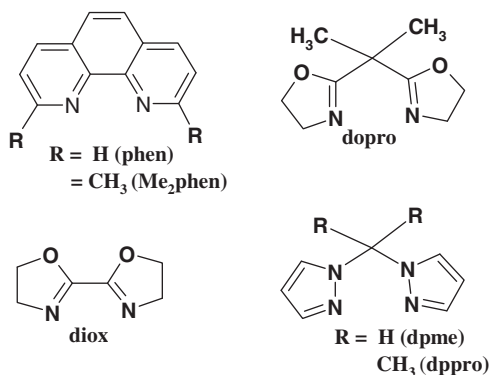


Figure 5. Structures for bidentate ligands reported from literature [16] for complexes containing the [Ru(terpy)(NN)(H₂O)]²⁺ cation.

properties of their coordinated bidentate ligands. The values of the second-order rate constants, k_2 , for the direct attack of the incoming nucleophiles at the metal center were calculated from slopes of the individual concentration dependence plots at 25°C. These are summarized in table 4. Included in table 4, for the purpose of looking at the complete trend, are the literature values for analogous ruthenium(II) aqua complexes all having an in-plane steric directing terpy of general form [Ru(terpy)(NN)OH₂]²⁺, where NN represents bidentate ligands, phen (1,10-phenanthroline), Me₂phen (2,9-dimethyl-1,10-phenanthroline), diox {di(1,3-oxazoline)}, dopro {2,2-di(1,3-oxazolinyl)propane}, and dppro {2,2-di(1-pyrazolyl)propane} [18]. The structures of the bidentate ligands whose complexes are listed in table 4 are given in figure 5.

4. Discussion

The ligand substitution behavior of octahedral ruthenium(II) complexes has been extensively studied [10 a, 18, 19]. The mechanism of substitution proceeds *via* a transition state which has dissociative interchange (I_d) character [10 b, 19, 20]. The absence of low-lying d orbitals preclude the formation of seven-coordinate encounter complexes at the ruthenium(II) metal center which would lead to an I_a -activated reaction pathway. In the I_d -activated encounter complex, the dissociation of the leaving group takes precedence and a dependence of the measured first-order rate constants on the concentration of the incoming nucleophiles is observed because in the intimate encounter complex, the metal begins to form a bond with a nucleophile in the outer sphere before the bond with the leaving group is fully broken [20]. Thus, the second-order kinetics observed in this study reaffirms what has been reported previously [20, 21], that the activation pathway for the substitution of aqua leaving groups by nucleophiles in octahedral ruthenium(II) complexes proceed *via* a dissociatively activated interchange mechanism [20].

A look at the reactivity data in table 4 shows that the tmen derivative reacts slightly faster {by factors of about 2 (tu) and 1.5 (dmtu)} than the bipy derivative when the strong thioureas are the incoming nucleophiles. To gauge our kinetic procedure, we repeated the substitution reaction of $\text{Ru}(\text{terpy})(\text{bipy})\text{OH}_2]^{2+}$ and CH_3CN as nucleophile. The rate constant obtained is $1.1 \times 10^{-4} (\text{mol L}^{-1})^{-1} \text{s}^{-1}$ and compares well with the value of $0.75 \times 10^{-4} (\text{mol L}^{-1})^{-1} \text{s}^{-1}$ reported by Bessel *et al.* [18]. However, on changing the structure of the bidentate ligand from bipy to tmen, the rate of substitution of the coordinated aqua ligand ($0.8 \times 10^{-4} (\text{mol L}^{-1})^{-1} \text{s}^{-1}$) by acetonitrile was invariant. Given the dissociative character of the substitution reaction and when one considers the structural differences that exist between the bipy and tmen complexes, a much more dramatic IPLE [10 b] would have been anticipated in the tmen complex. A similar dramatic enhancement in the substitutional reactivity (9.4×10^5) at a dissociatively activated octahedral geometry has been recorded by Takeuchi *et al.* [20 a] when the NN bidentate ligand was changed from 2,2-di(1-pyrazoyl)methane (dpme), a chelate with two hydrogens on its bridgehead carbon, to 2,2-di(1-pyrazoyl)propane (dppro), an analogous chelate with two methyl groups on its bridgehead carbon in $[\text{Ru}(\text{tpmm})(\text{NN})\text{H}_2\text{O}]$, where tpmm = tris-(pyrid-2-yl)methoxymethane, a three pronged pyridyl σ -donor. Similar spectacular changes in the rates of substitutions of the aqua leaving groups by acetonitrile were also observed in complexes of the type $[\text{Ru}(\text{II})(\text{NNN})(\text{dppro})\text{H}_2\text{O}]$, where dppro = {2,2-di(pyrazoyl-1-yl)propane} is a NN heteroscorpionic bidentate; NNN = (i) *mer*-terpy, a typical good π -acceptor ligand [18] and (ii) facially coordinated-tpmm (*fac*-tpmm) [10 b, 18, 20 a], a σ donor with three-pronged pyridyl units whose facial coordination to the metal center forced the bidentate to exert an out-of-plane ligand effect (OPLE) on the leaving group. For example, when Bessel *et al.* [10 b, 18, 20] changed the structure of the bidentate ligand from phen (projected group = H) to 2,9-Me₂phen (projected group = CH₃), a 660-fold increase in the reactivity of the latter ruthenium(II) was observed when the anchoring ligand was a *mer*-coordinated terpy. The most spectacular enhancement factor of about 1.9×10^7 was recorded when the exerting role of the dppro bidentate ligand was changed from an in-plane (by coordination of the anchoring planar *mer*-terpy complex) to an out-of-plane in the *fac*-tpmm complex [10 b, 18, 20 a]. In the latter complex, the facial-coordination of tpmm allowed the two pyrozyl rings of the dppro NN-bidentate ligand

to form a well-defined boat conformation, which positioned the propane bridgehead carbon and its hydrogens to interact closely with oxygen of the aqua leaving group, resulting in a dramatic increase in the rate of substitution [10 b].

What is common in the substitution reactions of these ruthenium(II) complexes is an unusually high sensitivity of the rates of their ligand-substitution reactions when slight changes are made in structures of the ligand backbone around the metal. This happens when either the atoms or ancillary groups on the bidentate ligands or IPLE/OPLE roles of the tridentate ligands are changed. Specifically, electrostatic interactions of the ancillary groups on the NN bidentate ligands render a “hetero scorpionatic” interactive “sting” [22, 23] on the bond between the metal center and the leaving group causing a labilization effect in the ground-state properties of the complex. As already stated these interactions are mainly repulsive and originate from the topology of the ancillary groups. The steric topology and hence the geometrical arrangement of the bidentate relative to the leaving group is modulated by coordination geometry of the tridentate ligand. For example, replacement of the *mer*-terpy ligand by *fac*-tpmm, which effectively switches the bidentate dppro ligand from exerting an IPLE to an OPLE, enhanced the scorpionatic effect of the bidentate ligand [10 b, 18, 20 a] (*vide supra*). In the *mer*-terpy complex, strong π -interactions affect the dppro, causing the bidentate to assume a more rigid conformation at its carbon bridgehead, pushing its dimethyl ancillary groups on its bridgehead carbon away from the leaving group. This rendered its scorpionatic effects less effective. In the *fac*-tpmm complex, the bidentate folded inward in a manner that positioned its dimethyl groups at the bridgehead carbon to interact strongly with the leaving group due to the inherent flexibility at its carbon bridgehead.

It is also possible that if hydrogens or ancillary groups on NN are correctly and closely positioned to oxygen of the aqua leaving group, they can form stable five- or six-membered cyclic structures *via* unconventional short hydrogen bonding contacts whose collective bipolar interactions can facilitate substitution of the leaving group. Such agostic interactions [23] exerted by closely positioned atoms or ancillary groups of NN chelates form part of the “invisible sting” effect of the tail on the leaving group.

When one looks at the steric topology of bipy and tmen, the repulsive forces and the collective effect of the scorpionatic interactions were expected to be stronger in the tmen complex than in the bipy complex, despite the methyl groups of the tmen ligand being located on the hind side relative to its *cis*-coordination. If Tolman’s cone angle of the tmen complex was determined, the four steric-imparting methyl groups would frame a larger angle over the metal center, comparable in magnitude to tertiary phosphines [24]. The collective impact of the steric interactions on the active site (the chloride/aqua leaving group) would be to weaken the Ru–Cl bond or to laterally bend the bond out of the expected colinearity of N_{bipy}, Ru, and Cl due to the repulsive forces of the properly positioned steric-imparting ancillary groups on the bidentate ligands. A check on the model structures of the two complexes and their phen analogues in table 2 confirm this proposition. The collective effect of the atoms or groups attached to the bidentate ligands is to repel the electron cloud of the Ru–Cl in a lateral or longitudinal fashion. For example, complexes of the substituted bidentates (2,9-Me₂phen, tmen) show that Ru–Cl is laterally bent from the expected co-linearity of N^{*trans*}_{bipy}–Ru–Cl, straining it away from the terpy. The lateral strain of the bond to the leaving ligand may result in high rates of substitution at its metal center. The high substitution reactivity of this complex has been reported by Bessel *et al.* [18].

The question that still needs to be answered for the reactions of the two complexes with CH_3CN as nucleophile is, why did the rate of substitution remain almost invariant when the steric topology of the bidentates was increased from the bipy to the tmen? To answer this completely, we need to first analyze the electronic and steric contributions of the co-ligands at the metal centers in the two complexes.

Data in table 1 reveal significant differences in the metrics of the two complexes in their ground states, signifying different electronic contributions due to their ligands. Of note is the trend in the calculated NBO charges (table 1) of Ru(II) which decreases in the order: $\text{tmen} < 2,9\text{-Me}_2\text{phen} < \text{phen} \approx \text{bipy}$ according to the decrease in the σ -donor capacity of the *cis*-coordinated bidentate ligands, a pump of the electron density at the Ru(II) metal center. In the tmen complexes, the positive σ -induction due to the four methyl groups on the ethylenediamine (en) backbone strengthen the σ -donor capacity of the *cis*-coordinated ligand through a σ -inductive effect. This lowers the electrophilicity of the Ru(II) in the order shown for the effective charges (table 1). Nucleophilic attack by incoming nucleophiles to form the bimolecular I_d -activated transition state is retarded, resulting in decreased rates of substitution of the leaving group. Unlike tmen, bipy and its aromatic analogues withdraw electron density from ruthenium(II) through π -back bonding, making the center more positively charged in the transition state. As a result, calculated charges on Ru(II) (table 1) are relatively higher than in the tmen complex. In the bimolecular activated transition state of the I_d substitution, the π -acceptability of the bidentate ligand due to the common conjugated π -backbone causes Ru(II) to be highly electrophilic, facilitating departure of the chloride/aqua leaving groups. This is further supported by the mapping of their HOMOs which extend to the aromatic rings of the bidentate ligands (table 2).

However, when the calculated bond lengths of the Ru–Cl were ranked, the order was $\text{tmen} < \text{phen} \approx \text{bipy} < 2,9\text{-Me}_2\text{phen}$ revealing an unusual shortening in the Ru–Cl bond length of the tmen complex. It seems that the electronic effect of the *cis*-coordinated NN is modulated by the *mer*-terpy which is predominantly π -accepting. In fact the strong repulsive forces which exist between ancillary groups of the bulky tmen and the extended π -electron cloud of *mer*-terpy repel the four methyl groups away from the favorable axial projection toward the leaving group. This weakens the scorpionatic effect of the ligand, leading to retarded rates of substitution. In an octahedral Ru(II) containing a *mer*-terpy, the terpy exerts a profound π -repulsive effect whereby its extended π -conjugated backbone fans the electron density of ancillary groups on the bidentate ligand away from the leaving group conferring stereoelectronic rigidity in their facial coordination. As a result, the calculated Ru(II)–N_{trans} bond length (Å) increases in the order of the repulsive forces and hence the steric bulky of the bidentate as $\text{bipy} (2.126) \approx \text{phen} (2.136) < 2,9\text{-Me}_2\text{phen} (1.197) < \text{tmen} (2.203)$. As the N_{trans} and Cl[−] share the same *p*-orbital of the metal center, a weakened Ru(II)–N_{trans} bond strengthens the bond between the metal center and the leaving group. The steric-induced weakening of Ru(II)–N_{trans} in the tmen complex strengthens the *trans* bond between the metal and the leaving group, resulting in the unusual strengthening (shortened bond length) of Ru–Cl.

Since the repulsive forces are mutual, similar distortions are expected on the planarity of terpy especially in bidentate ligands having the greatest cone angles [24] in their steric topologies. This is observed in the calculated model structure of the tmen complex. The strong π -acceptability of the *mer*-terpy is significantly compromised due to distortions in the planarity of its molecular orbitals. The electron density due to the

σ -inductive effects of tmen toward Ru(II), which has been noted to reduce its electrophilicity (reduced NBO charge, table 1, *vide supra*), is unaffected by the π -acceptability of the distorted *mer*-terpy ligand. The consequent effect of inefficient mopping of electron density from the metal center by the distorted *mer*-terpy is to retard the approach of the incoming nucleophiles, thus leaving the *cis* σ -effect due to the tmen ligand to take over the control of the reactivity of Ru(II). The collective effect of the two mutually interacting non-leaving ligands of this complex is to retard the approach of the incoming groups through a dominant *cis* σ -effect from tmen toward the metal center. A similar retardation in the rate of substitution due to the *cis*- σ effect of the ligand on the lability of the leaving group has been reported for a Pt(II) square-planar geometry in our previous work [25]. As already stated, the presence or lack of mutually exerted repulsive interaction between the coligands is the reason for a dramatic change in the rates of substitutions of the leaving groups at the octahedrally coordinated Ru(II) complexes, when the tridentate ligand was switched from the turgid-imparting *mer*-terpy (IPLE) to the flaccid-exerting *fac*-tpmm (OPLE) in two complexes bearing a common dppro [10 b, 20 a]. Thus, it can be speculated that replacement of the *mer*-terpy (IPLE) by *fac*-tpmm (OPLE) while maintaining the bidentate ligand as tmen should yield an even more dramatic reactivity enhancement factor than that recorded (1.9×10^7) for the analogous complexes bearing a common dppro as the bidentate ligand [10 b, 20 a] due to the superior steric topology of the former bidentate.

Another possible reason for the unusually low reactivity of the tmen complexes is that the steric-imparting methyl groups are located on the hind side of the facial coordination of the bidentate ligands and the methyl groups may interfere with direct approach of the incoming CH_3CN toward the metal center by exerting repulsive forces [26] or through the formation of temporal agostic hydrogen bonding short contacts [21] between their hydrogens and the nucleophile. However, when a favorable projection on the interacting groups of the bidentate ligand is achieved by an anchoring coligand (terpy), the combined ligand effect of the bidentate and the terpy is dominated by the strong repulsive forces between the extended π -conjugated backbone of the terpy and the electron density of ancillary groups.

When one looks at the complete reactivity trend for the tmen and the bipy derivatives with the three nucleophiles, the sulfur donors were better nucleophiles than CH_3CN toward Ru(II), in line with the high nucleophilicity of the sulfur nucleophiles over the platinum group metals. If the rate constants from this study and other previous studies [10 b, 18, 20] for the substitution of leaving group by CH_3CN is ranked by the ligand effect of the bidentate ligand in ruthenium(II) complexes, the order is $\text{NN} = \text{dppro} < \text{dopro} < \text{phen} \approx \text{bipy} < \text{tmen} < \text{diox} < 2,9\text{-Me}_2\text{phen}$. This order reflects the steric and electronic properties in an octahedral coordination sphere where meridionally coordinated terpy enacts stereoelectronic rigidity on the bidentate ligands in addition to providing a pump of excess electron density at the metal (where distortion in the planarity is minimal), which would make breaking of the bond more difficult in the encounter complex of an I_G -activated pathway. In cases where ancillary groups of the bidentate ligand are in close proximity to the leaving group, such as in 2,9- Me_2phen , their scorpionatic effect (steric effects) predominates leading to dramatic changes in substitution. This steric effect is enhanced when the terdentate ligand imparts an out-of-plane exerting role on the bidentate ligand as reported for *fac*-tpmm complexes.

5. Conclusion

This study has shown that for octahedral ruthenium(II) complexes, with strong π -acceptor groups (such as planar terpy) meridionally coordinated, stereoelectronic rigidity is enacted on their co-bidentate ligands. The π -acceptors assist in withdrawal of electron density from the metal center through π -back bonding. When the anchored bidentate ligand has the right structural geometry to project its steric imposing groups in close proximity to the metal center and the leaving group (as found in the optimized structure of 2,9-Me₂phen), then dramatic changes in the substitutional reactivity at the metal is recorded from the scorpionatic effect of the ancillary methyl groups. However, this kind of scorpionatic effect becomes less important if the steric features of the *cis*-coordinated bidentate ligand are located at its hind (as was the case with the tmen bidentate ligand), especially if the tridentate ligand has a repelling π -backbone as exemplified by *mer*-terpy. In the tmen complex, the four methyl groups can also interact agostically with oncoming nucleophiles, thereby slowing their rates of approach to the inner shell. In all cases, lower rates are expected.

The second-order kinetics and dependence of the rate on the nature of the incoming group reiterate the bimolecular character of the transition state since the data fit a reaction coordinate characteristic of a bond-making process.

Acknowledgments

The authors gratefully acknowledge financial support from the University of KwaZulu-Natal, The South African National Research Foundation. We are also grateful to the Alexander van Humboldt Foundation for the donation of the UV-Vis spectrophotometer.

References

- [1] C.X. Zhang, S.J. Lippard. *Curr. Opin. Chem. Biol.*, **7**, 481 (2003).
- [2] X. Anon. *Drug Res. Dev.*, **3**, 67 (2002).
- [3] B. Sanna, M. Deidda, G. Pintus, B. Tadolini, A.M. Bennardini, G. Sava, C. Ventura. *Arch. Biochem. Biophys.*, **403**, 209 (2002).
- [4] (a) M.J. Clarke. *Coord. Chem. Rev.*, **236**, 209 (2003); (b) N. Gupta, N. Grover, G.A. Neyhart, P. Singh, H.H. Thorp. *Inorg. Chem.*, **33**, 5779 (1993); (c) N. Grover, H.H. Thorp. *J. Am. Chem. Soc.*, **113**, 7030 (1991); (d) A.E. Friedman, J.C. Chambron, J.P. Sauvage, N.T. Turro. *J. Am. Chem. Soc.*, **112**, 4960 (1990); (e) N. Grover, N. Gupta, P. Singh, H.H. Thorp. *Inorg. Chem.*, **31**, 2041 (1992); (f) C.G. Coates, L. Jacquet, J.J. McGarvey, S.E.J. Bell, A.H.R. Al-Obaidi, J.M. Kelly. *J. Am. Chem. Soc.*, **119**, 7130 (1997); (g) I. Greguric, J.R. Aldrich-Wright, J.D. Collins. *J. Am. Chem. Soc.*, **119**, 3621 (1997); (h) I. Hag, P. Lincoln, D. Suh, B. Norden, B.Z. Chowdhry, J.B. Chaires. *J. Am. Chem. Soc.*, **117**, 4788 (1995); (i) Y. Xiong, X. Xe, X. Zou, J. Wu, X. Chen, L. Ji, R. Li, J. Zhou, K. Yu. *J. Chem. Soc., Dalton Trans.*, **19** (1999). (j) F.M. Forey, F.R. Keene, J.D. Collins. *J. Chem. Soc., Dalton Trans.*, 2825 (2001).
- [5] B.P. Sullivan, J.M. Calvert, T.J. Meyer. *Inorg. Chem.*, **19**, 1404 (1980).
- [6] (a) J.M. Calvert, R.H. Schmehl, B.P. Sullivan, J.S. Facci, T.J. Meyer. *Inorg. Chem.*, **22**, 2151 (1983); (b) C. Cheng, J.G. Goll, G.A. Neyhart, T.W. Welch, P. Singh, H. Thorp. *J. Am. Chem. Soc.*, **117**, 2970 (1995).
- [7] C. Ho, C. Che. *J. Chem. Soc., Dalton Trans.*, 967 (1990).
- [8] (a) D. Jaganyi, A. Hofmann, R. van Eldik. *Angew. Chem., Int. Ed.*, **40**, 680 (2001); (b) D. Jaganyi, F. Tiba. *Transition Met. Chem.*, **28**, 803 (2003).

- [9] (a) R.A. Friesner. *Chem. Phys. Lett.*, **116**, 539 (1985); (b) R.A. Friesner. *Ann. Rev. Chem. Phys.*, **42**, 341 (1991); (c) Spartan 04, Wavefunction, Inc., 18401 von Karman Avenue, Suite 370, Irvine, CA 92612, USA; Q-Chem, Inc., The Design Center, Suite 690, 5001 Baum Blvd., Pittsburgh, PA 15213, USA (2004), Available online at: <http://www.wavefun.com/> (accessed November 8, 2009); (d) K. Kong, C.A. White, A.I. Krylov, C.D. Sherrill, R.D. Adamson, T.R. Furlani, M.S. Lee, A.M. Lee, S.R. Gwaltney, T.R. Adams, C. Ochsenfeld, A.T.B. Gilbert, G.S. Kedziora, V.A. Rassolov, D.R. Maurice, N. Nair, Y. Shao, N.A. Besley, P.E. Maslen, J.P. Dombroski, H. Daschel, W. Zhang, P.P. Korambath, J. Baker, E.F.C. Byrd, T. van Voorhuis, M. Oumi, S. Hirata, C.P. Hsu, N. Ishikawa, J. Florian, A. Warshel, B.G. Johnson, P.M.W. Gill, B.G. Pople. *J. Comput. Chem.*, **21**, 1532 (2000); (e) A.D. Becke. *J. Chem. Phys.*, **98**, 5648 (1993); (f) C. Lee, W. Yang, R.G. Parr. *Phys. Rev.*, **B37**, 785 (1998); (g) P.C. Hariharan, J.A. Pople. *Chem. Phys. Lett.*, **16**, 217 (1972); (h) P.J. Hay, W.R. Wadt. *J. Chem. Phys.*, **82**, 299 (1985).
- [10] (a) D.P. Rillema, D.S. Jones. H.A. Levy. *J. Chem. Soc., Chem. Commun.*, 849 (1979); (b) M.H.V. Huynh, J. Smyth, M. Wetzler, B. Mort, P.K. Gong, L.M. Witham, D.L. Jameson, D.K. Geiger, J.M. Lasker, M. Charepoo, M. Gornikiewicz, D.G. Churchill, M.R. Churchill, K.J. Takeuchi. *Angew. Chem. Int. Ed.*, **40**, 4469 (2001).
- [11] (a) P.A. Adcock, F.R. Keene, R.S. Smythe, M.R. Snow. *Inorg. Chem.*, **23**, 2336 (1984); (b) S.C. Rasmussen, S.E. Ronco, D.A. Mlsna, M.A. Biladeau, W.T. Pennington, J.W. Kolis, J.D. Petersen. *Inorg. Chem.*, **34**, 821 (1995).
- [12] J.L. Walsh, R. McCracken, A.T. McPhail. *Polyhedron*, **17**, 3211 (1998).
- [13] C. Bonnefous, A. Chouai, R.P. Thummel. *Inorg. Chem.*, **40**, 5851 (2001).
- [14] V.J. Catalano, R.A. Heck, C.E. Immoos, A. Ohman, M.G. Hill. *Inorg. Chem.*, **37**, 2150 (1998).
- [15] H. Nagao, T. Mizukawa, K. Tanaka. *Inorg. Chem.*, **33**, 3415 (1994).
- [16] (a) A. Gerli, J. Reedjik, M.T. Lakin, A.L. Spek. *Inorg. Chem.*, **34**, 1836 (1995); (b) K.J. Takeuchi, M.S. Thompson, D.W. Pipes, T.J. Meyer. *Inorg. Chem.*, **23**, 1845 (1984).
- [17] T.G. Appleton, J.R. Hall, S.F. Ralph, C.S.M. Thompson. *Inorg. Chem.*, **23**, 3521 (1984).
- [18] C.A. Bessel, J.A. Margarucci, J.H. Acquaye, R.S. Rubino, J. Crandall, A.J. Jircitano, K. Takeuchi. *Inorg. Chem.*, **32**, 5779 (1993).
- [19] (a) R.A. Leising, J.S. Ohman, K.J. Takeuchi. *Inorg. Chem.*, **27**, 3804 (1988); (b) H. Taube. *Comments Inorg. Chem.*, **1**, 17 (1981).
- [20] (a) M.H.V. Huynh, J.M. Lasker, M. Wetzler, B. Mort, L.F. Szczepura, L.M. Witham, J.M. Cintron, A.C. Marschilok, L.J. Ackerman, R.K. Castellano, D.L. Jameson, M.R. Churchill, A.J. Jircitano, K.J. Takeuchi. *J. Am. Chem. Soc.*, **123**, 8780 (2001); (b) M.H.V. Huynh, L.M. Witham, J.M. Lasker, M. Wetzler, B. Mort, D.L. Jameson, P.S. White, K.J. Takeuchi. *J. Am. Chem. Soc.*, **125**, 308 (2003).
- [21] (a) R.E. Shepherd, H. Taube. *Inorg. Chem.*, **12**, 1392 (1973); (b) S.S. Iseid, H. Taube. *Inorg. Chem.*, **15**, 3070 (1976); (c) T. Matsubara, C. Creutz. *Inorg. Chem.*, **18**, 1956 (1979); (d) L.R. Allen, P.P. Craft, B. Durham, J. Walsh. *Inorg. Chem.*, **26**, 53 (1987); (e) C.H. Langford, W.R. Muir. *J. Am. Chem. Soc.*, **89**, 3141 (1967).
- [22] S. Trofimenko. *J. Am. Chem. Soc.*, **89**, 6288 (1996).
- [23] Ž.D. Bugarčić, G. Liehr, R. van Eldik. *J. Chem. Soc., Dalton Trans.*, 2825 (2002).
- [24] (a) C.A. Tolman. *J. Am. Chem. Soc.*, **92**, 2953 (1970); (b) C.A. Tolman. *Chem. Rev.*, **77**, 313 (1977); (c) C.A. Tolman. *J. Chem. Educ.*, **63**, 199 (1986).
- [25] (a) A. Hofmann, D. Jaganyi, O.Q. Munro, G. Liehr, R. van Eldik. *Inorg. Chem.*, **42**, 1688 (2003); (b) D. Jaganyi, D. Reddy, J.A. Gertenbach, A. Hofmann, R. van Eldik. *J. Chem. Soc., Dalton Trans.*, 299 (2004).
- [26] T.L. Brown. *Inorg. Chem.*, **31**, 1286 (1992).